Since January 2020 Elsevier has created a COVID-19 resource centre with free information in English and Mandarin on the novel coronavirus COVID-19. The COVID-19 resource centre is hosted on Elsevier Connect, the company's public news and information website.

Building and Environment 210 (2022) 108728

Contents lists available at ScienceDirect

Building and Environment

journal homepage: www.elsevier.com/locate/buildenv

Experimental testing of air filter efficiency against the SARS-CoV-2 virus: The role of droplet and airborne transmission

Cesare Saccani [a,*], Alessandro Guzzini [a], Caterina Vocale [b], Davide Gori [c], Marco Pellegrini [a], Maria Pia Fantini [c], Alessandra Primavera [b]

[a] Department of Industrial Engineering (DIN), University of Bologna, Viale del Risorgimento 2, 40136, Bologna, Italy
[b] Regional Reference Center for Microbiological Emergencies (CRREM), Microbiology Unit, IRCCS, Azienda Ospedaliero-Universitaria di Bologna, Via Albertoni 15, 40138, Bologna, Italy
[c] Department of Biomedical and Neuromotor Sciences (DIBINEM), University of Bologna, via San Giacomo 12, 40126, Bologna, Italy

ARTICLE INFO

Keywords:
Coronavirus disease 2019
SARS Coronavirus
COVID-19
Heating ventilation and air conditioning systems
Air filters
Experimental testing

ABSTRACT

Verifying the capacity of different types of air filters to stop the propagation of the SARS-CoV-2 virus has become a strategic element to contain viral spreading in enclosed spaces. This paper shows the results of experimental tests about the capacity of different commercial filter grades to stop SARS-CoV-2 propagation using inactivated virions. In the first test, the obtained results showed that the F8 filter blocks SARS-CoV-2 propagation if it encounters a flow devoid of liquid phase, i.e., a biphasic flow that can wet the filtering material. On the contrary, as shown in the second test, the SARS-CoV-2 virus propagates through the F8 filter if the droplet content in the air flow is enough to wet it. In these operational conditions, i.e., when the filter is wet by a flow with a high droplet content, the absolute H14 filter was also shown to fail to stop the transmission of the SARS-CoV-2 virus. Lastly, in the third test, the viral load was shown to be stopped when the pathway of the infected droplet is blocked.

1. Introduction

Prevention, protection and treatment are essential elements in a welfare system that aims to ensure people's health and safety. The containment strategy applied during the COVID-19 pandemic, particularly in the early stages, included the adoption of prevention strategies based on non-pharmaceutical interventions, such as lockdown measures of varying degrees of strictness and duration. The health crisis associated with the COVID-19 pandemic therefore also transformed into an economic and social crisis [1–6]. While it is true that vaccination and the development of medical treatments are the solution to the spreading of the pandemic, it is equally true that, in the pandemic spread phase, no completely appropriate prevention and protection systems other than lockdowns were applied. To develop alternative systems, a good knowledge of the mechanisms underlying infection among people would have been required.

As an example, the hypothesis that being in enclosed spaces and carrying out activities there could increase the chances of contagion spreading was investigated by the scientific community [7,8]. It is believed that more than one outbreak originated in confined spaces: call centers [9], restaurants [10], buses [11,12], churches [13], meat processing plants [14] are but a few examples [15]. Although trade associations have published protocols and guidelines for the correct use of air conditioning facilities [16–18], having numerous people carry out activities in confined spaces was generically classified as "at risk", without developing tools for the quantification or control of such risk.

One of the proposed solutions to minimize risk, if ventilation is not possible [19], is the use of high efficiency filters [20] or, preferably, High Efficiency Particulate Air (HEPA) filters. In compliance with ISO 29463-1 [21], HEPA filters guarantee a filtering efficiency equal to or above 99.95% of particles in the 0.1–0.3 μm range. The lower limit overlaps with the diameter of the SARS-CoV-2 virion, which is between 60 nm and 150 nm [22]. However, as it is not possible to install these filters in all existing systems, other solutions have been recommended, such as the adoption of filters that are at least class F8 (EN 779-2012), i.e., filters with an average 95% filtering efficiency for particles with a 0.4 μm aerodynamic diameter. However, even if some assumptions exist in the literature [23,24], the experimental validation is still awaited.

To investigate the performance of different filters' grade against SARS-CoV-2 is a very challenging task. In fact, even though the

* Corresponding author.
E-mail address: cesare.saccani@unibo.it (C. Saccani).

https://doi.org/10.1016/j.buildenv.2021.108728
Received 22 October 2021; Received in revised form 8 December 2021; Accepted 22 December 2021
Available online 27 December 2021

efficiency of commercial filters is known and measured by standardized tests, the conditions that verify when installed in real world are difficult to be simulated in experimental tests. First of all, since SARS-CoV-2 virions are emitted through droplets by infected subjects, droplets size distribution should be reproduced to simulate the emission source. Unfortunately, no agreement exists in the literature [25]. Secondly, since droplets are liquid and not solid particles, evaporation should also be considered in the experimental modelling to take into account of the mass transfer phenomenon that depends on a lot of parameters such as, but not limited to, air temperature and humidity. Despite dedicated research programs are expected to cover these gaps, no time is now available. A definitive answer on the capability of commercial filters to stop or not the SARS-CoV-2 propagation is required by the community as soon as possible.

Trying to give an answer, some authors simply hypothesized the capacity of HEPA filters to stop the propagation based on the nominal performance of the filters and on the size of SARS-CoV-2 virions [26–30]. Others carried out tests to assess the efficacy of the filters but used bacteria or viruses that were not SARS-CoV-2. Among them [31], tested four types of filters for residential application, i.e., MERV5, MERV12, MERV13 and MERV14 (ANSI/ASHRAE 52.2–2012) which correspond, respectively, to G4, M6, F7 and F8 filters (EN 779-2012), using MS2, a single-strand RNA bacteriophage virus with a diameter of 27 nm. They found that the highest efficiency filter, MERV14, effectively blocks viral particles. [32] tested the efficacy of air purifiers with HEPA14 filters in removing viral content in infected aerosol. The reduction in viral concentration at the device exit was found to be of between 99.9974 and 99.9999%. In this case as well, the virus used was not SARS-CoV-2 but the phiX174 bacteriophage, a single-strand DNA virus with a diameter of approximately 30 nm. In both cases, the aerodynamic diameter of the virus (of the viral particle) was below that of the SARS-CoV-2 virus. In the past other researchers have been interested in investigating the capacity of filters against viruses and bacteria. [33] firstly described and applied a method to check the efficacy of HEPA filters against infected aerosols. Specifically, in their tests, they used the bacteriophage *T1* (a virus with 0.1 μm average diameter) and *Bacillus subtilis* (a black-pigmented bacterium with a 1 μm average diameter), and found that the filters' protection against submicron aerosols was excellent. [34] tested the efficacy of commercial HEPA filters in terms of removal of the *Stremptomyces virginiae* bacterium (average diameter: 50 nm) from the air in the standard conditions of a white room. They found the filters' efficiency was above 99.996%. [35] tested two filter configurations (EU6 + EU9 and EU6 + S, in compliance with DIN 24185 and DIN 24184, which correspond, respectively, to M6 + F9 and M6 + H13) to assess the efficacy in relation to the *minute virus of mice* (MVM), which has an average diameter between 22 and 26 nm. The test results confirmed the efficacy of both filter configurations. [36] checked the efficacy of MERV14 filters (which correspond to F8 filters), used for sampling viruses and bacteria. They used *Bacillus anthracis* (length: 3–5 μm, width: 1–1.2 μm), SARS coronavirus (average diameter between 50 nm and 80 nm), the *Respiratory Syncytial Virus* (average diameter between 150 nm and 250 nm) and the *Smallpox* virus (average diameter: 200 nm). Specifically, the capture efficiency for *Bacillus anthracis* was 96.5% ± 1.5%, while no data was provided by the authors for the viruses because no viable pathogens were detected in the section downstream of the filter. [37] checked the performance of filters normally used for sampling viruses and bacteria with a diameter in the 10–900 nm range. Lastly, [38] tested the combination of G4 + F9 filters and the M6, F8–F9 filters in terms of efficacy against aerosols infected with six different pathogens: *Equine Arteritis Virus* (AEV) (average diameter between 40 nm and 60 nm), *Staphylococcus aureus* (average diameter between 0.5 μm and 1.5 μm), *Porcine Reproductive and Respiratory Syndrome Virus* (PRSSV) (average diameter approximately 60 nm), *Bovine Enterovirus 1* (BEV) (average diameter between 25 nm and 30 nm), *Actinobacillus pleuropneumoniae* (APP) (maximum width: approximately 0.5 μm, length: 1.4 μm) and *Mycoplasma hyorhinis* (average diameter approximately 450 nm). However, these research activities were not performed during a pandemic emergency.

To identify the best strategy against SARS-CoV-2 propagation, the local public transport company, TPER (Trasporto Passeggeri Emilia Romagna) S.p.A., funded and supported a research program aimed at providing guidelines for prevention and control measures in public transport settings in the context of SARS-CoV-2 infection. Among the activity, since several questions were raised by the community about the ability of air filters to stop or not SARS-CoV-2 propagation, an answer based on scientific evidence was quickly required.

This piece of scientific evidence would have a considerable impact also on other activities carried out in enclosed spaces. As reported by (Wenke et al., 2017) and in (REHVA, 2020), HEPA filters cannot always be installed in existing air conditioning systems, either because of size issues or of running costs. This makes it particularly important to understand whether the SARS-CoV-2 virus can or cannot be stopped by commercial filters less performing than HEPA filters.

Given these premises, this paper includes the results obtained during a number of experimental tests to validate if cabin air filters and air filters of the G4, M5, F8 and H14 type can stop SARS-CoV-2 propagation. Since the tests were performed during the second pandemic wave (November–December 2020), they were carried out in the Regional Reference Centre for Microbiological Emergencies (CRREM), Microbiology Unit of the IRCCS Policlinico di Sant'Orsola research hospital. The tests used SARS-CoV-2 as pathogen. Because there are no standard protocols in the literature, in addition to the experimental results, this paper describes the methodology developed to carry out the tests safely and the equipment designed and built by the Industrial Engineering Department (DIN) of the University of Bologna.

2. Materials and methods

2.1. Description of the experimental device

To execute the tests, an experimental device was designed and built to be used in a Biosafety Level-3 (BLS-3) laboratory with controlled access in the CRREM laboratory. The device is made up of two main elements: i) a tunnel with multiple filtering stations, and ii) a vacuum pump. The tunnel and pump are connected by a flexible hose supplied by the pump's manufacturer, with attachment points and needle valve to regulate flow. After testing, the tunnel was kept at lower pressure for the purpose of: i) preventing the release of hazardous substances into the environment during testing, and ii) avoiding any leaks of lubricating oil from the pump which would unavoidably occur if the device were pressurised. Specifically, the chosen pump's characteristics are listed in Table 1. The material chosen to build the device structure was polyvinylchloride (PVC).

Two configurations were created for the small-scale testing device.

The first configuration is shown in the diagram in Fig. 1, while Fig. 2 is a photo of it. The air, extracted by the vacuum pump, first encounters the solution containing inactivated SARS-CoV-2 in the section marked as "A". To that end, in this section, a mesh was included, so that the solution containing the inactivated virus can be deposited safely using a syringe (Fig. 3). In this configuration, the viral solution can be "launched" onto the downstream filters. The use of a syringe for the introduction of the inactivated SARS-CoV-2 solution was favoured over a spray to minimize

Table 1
Vacuum pump's nominal characteristics.

Characteristic	Value
Nominal flow rate, [liter/min]	30
Final vacuum, [mbar]	0.005
Electrical power, [kW]	0.18
Electrical voltage, [V]	220–240
Weight, [kg]	5

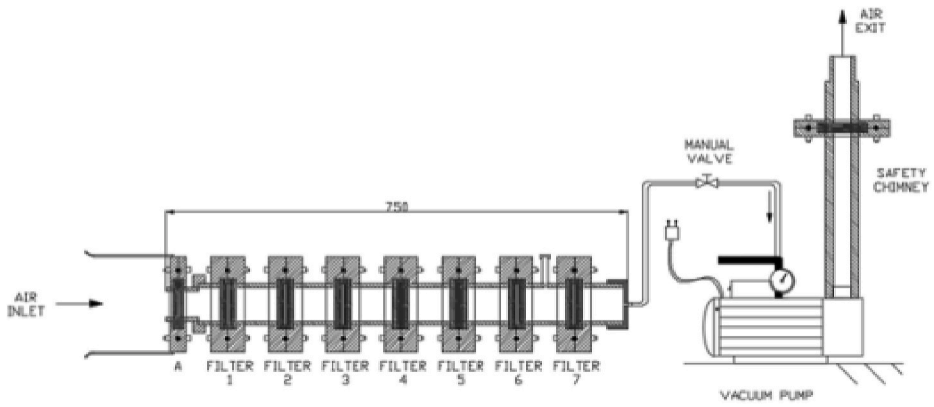

Fig. 1. Schematic drawing of the test bench for testing seven filters.

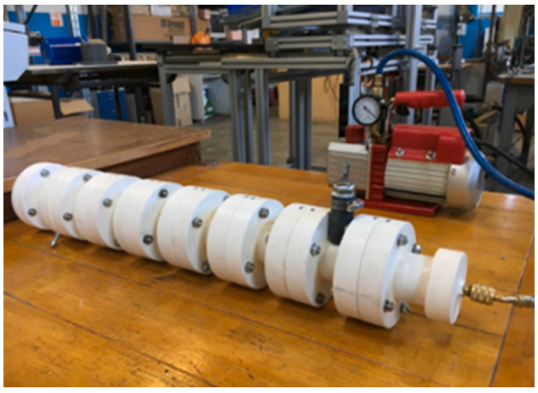

Fig. 2. The test device ready for use.

the risks related to the possible formation and release of aerosols from the tunnel during testing. Additionally, at the tunnel entrance, a specifically-designed collar was installed to provide the operator with extra protection (Fig. 3).

With regard to Fig. 4, downstream of section A (the first section the contaminated flow encounters), the flow inside the tunnel passes through, in sequence, seven filtering stations, each with increasing filtering efficiency, labelled in Fig. 4 with numbers 1 to 7: the efficiency of the filters installed in section number 7 is greater than of that installed in section number 6 and so on for upstream sections. Each filtering station was made by connecting two bolted flanges. Additionally, an O-ring and two rubber sealing washers were included to prevent the entry of external air into the tunnel. The filters described below were installed in stations 1 to 7. In positions 1 to 3, the filters installed were cabin air filters, of the sort used in air conditioning units in TPER S.p.A. vehicles. These filters (provided by the transport company) are installed on approximately 80% of their fleet. A polyester fiber filter (similar in structure to the previous filters) was installed in position 4. Greater efficiency filters were installed in positions 5 and 6, i.e., an F8 filter (compliant with EN 779) and a H14 filter (compliant with EN 1822-1). An absolute filter made of high purity quartz microfiber was installed in position 7 to block any residual SARS-CoV-2 that had not been captured by the upstream filters.

The sequence of the first configuration, related to Figs. 2 and 4, is:

- Filter 1: Expanded polyurethane filter installed in the transport company's vehicles
- Filter 2: Pleated filter installed in TPER vehicles
- Filter 3: Pleated filter installed in TPER vehicles
- Filter 4: EN 779 compliant polyester fiber G4 filter
- Filter 5: EN 779 compliant F8 fine filter

Fig. 3. A detail of the aqueous solution's entry point and of the protective collar.

- Filter 6: EN 1822-1 compliant high efficiency H14 filter
- Filter 7: Absolute filter

An exit duct with a second absolute filter was installed downstream of the pump, as shown in Fig. 5. In this case as well - as applied to the filter in position 7 - the aim is to guarantee extra safety, i.e., to prevent any accidental release of SARS-CoV-2 downstream of the pump, including through the release of the pump's (contaminated) lubricating oil.

The second configuration of the testing device is shown in Fig. 6. This configuration was used to validate the results obtained from the previous test and to test the filters that gave a negative result in two different operational conditions. Specifically, the "tunnel", i.e., the multi-stage filtering set, designed and built after analyzing the results of the first test, included a series of just two filtering stations, containing the F8 and

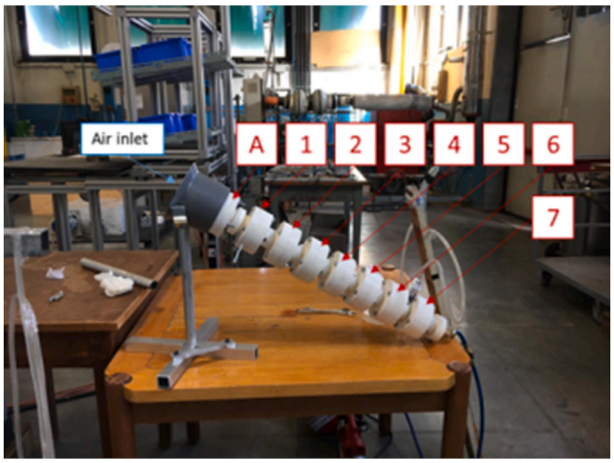

Fig. 4. The first tunnel to be built for the experimental campaign.

Fig. 5. The downstream chimney installed on the NPAV30 vacuum pump.

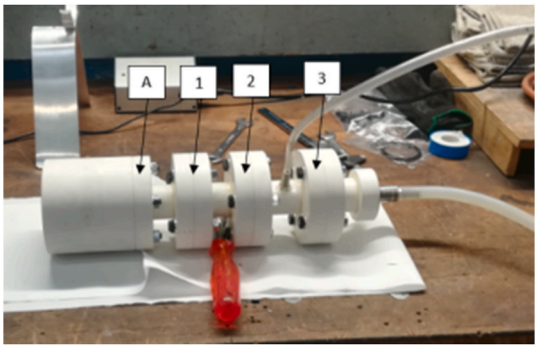

Fig. 6. The second tunnel, which was built to validate the results of the first test.

H14 filters. The station containing the absolute filter was inserted downstream of these filters.

With regard to Fig. 6, downstream of section A (which was not changed), the flow inside the tunnel passes through, in sequence, three filtering stations, each with increasing filtering efficiency, labelled with numbers 1 to 3, built as in the first configuration. The following filters were installed: the F8 filter in station 1 and the H14 filter in station 2. Lastly, for the same reason that applies to configuration 1, the absolute filter was positioned in station 3, which here is the device's last filtering station before the vacuum pump. In this case as well, downstream of the pump, the exit duct was protected by a second absolute filter, as shown in Fig. 5.

The sequence of the second configuration, related to Fig. 6, is:

- Filter 1: EN 779 compliant F8 fine filter
- Filter 2: EN 1822-1 compliant high efficiency H14 filter
- Filter 3: Absolute filter

2.2. *Description of the experimental tests*

The three tests described below were performed in the experimental campaign. Before discussing the applied methodology, it is important to specify that: i) the duration of the tests was limited to less than 1 h (more or less half an hour), and ii) the injection of the solution containing inactivated SARS-CoV-2 in the testing device was very quick when the tests were started.

2.2.1. *First test*

Configuration 1 was used in the first test (Fig. 1). After switching on the vacuum pump at the beginning of the test, the solution containing inactivated SARS-CoV-2 was injected (via syringe) on the metal mesh in the station labelled "A" in Fig. 4. Referring to Figs. 2 and 7, the air, extracted by the vacuum pump, enters the tunnel and comes into contact with the solution in station A, which is launched in the axial direction. The air flow, which is at room temperature and relative humidity when entering the system, after the evaporation of the liquid solution (at the same temperature as the air in the room), undergoes an isenthalpic process that leads to saturation, i.e., its relative humidity (RH) reaches 100%, with temperature drop to the dew point. The tunnel therefore was maintained operational (with air extraction) for the time needed for the viral solution injected inside to evaporate completely. Lastly, to ensure the correct introduction of the droplets inside the tunnel, the device was tilted during the test, as shown in Fig. 7.

2.2.2. *Second test*

The second configuration was used in the second test (Fig. 6). In station A, the metal mesh onto which the viral solution was positioned in the first test is replaced by a demister, onto which the viral solution is inserted, using a syringe, in an axial direction. The purpose of the demister is to ensure the homogeneous distribution of the liquid in the entry section. Compared to the first test, a different procedure was used, which is shown schematically in Figs. 8–10. Referring to the pictures, immediately after introducing the infected solution in the aspiration section (Fig. 8), uncontaminated water was injected between sections 2 and 3, i.e., between the H14 filter and the absolute filter, in order to wet their surfaces (Fig. 9). The tunnel was then moved to a vertical position, with the aspiration section on top, so that the infected liquid (injected into the demister in position A) could percolate towards the next sections (Fig. 10). The aim of the second test was to simulate a filter in a humidity-oversaturated environment, i.e., in the same conditions that would occur if it were reached by enough droplets to wet it.

2.2.3. *Third test*

The second configuration was used in the third test (Fig. 6). Station A was prepared as shown in Fig. 11. Specifically, the fluid (radially inserted from above using an insulin syringe) percolated through the

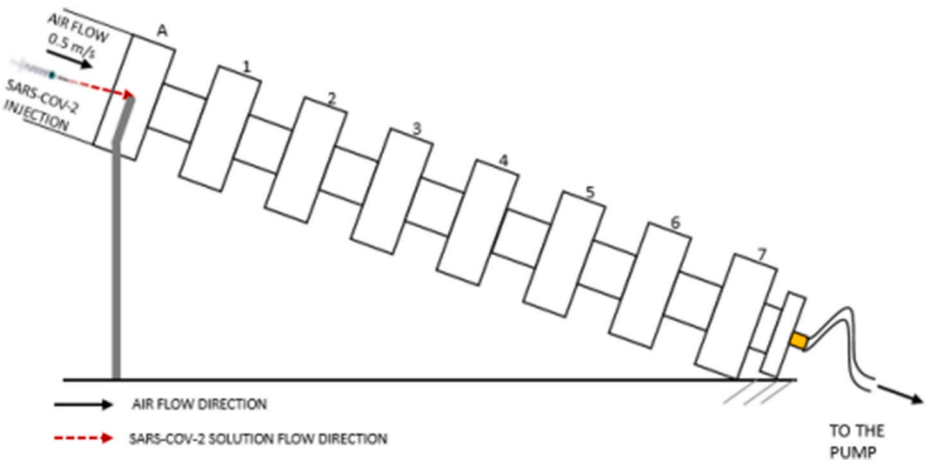

Fig. 7. Configuration and positioning implemented during the first test. The test bench was kept in a slightly inclined position during the experimental test to ensure the droplets moved in from the top to the bottom.

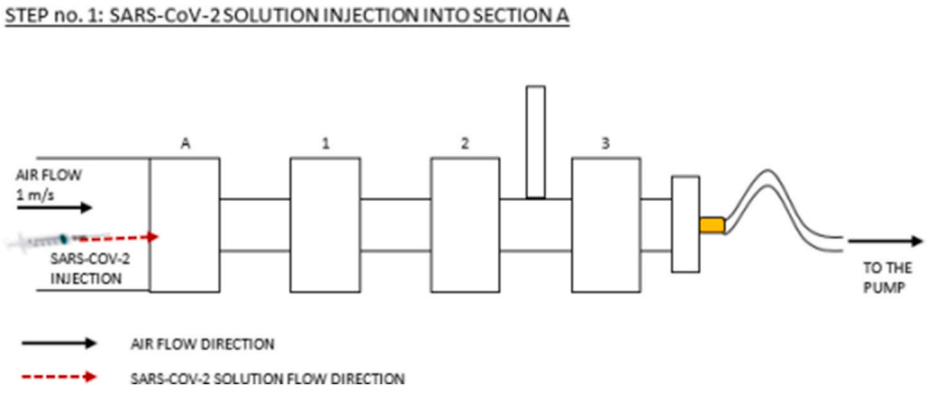

Fig. 8. First step of the second test: injection of the SARS-CoV-2 solution.

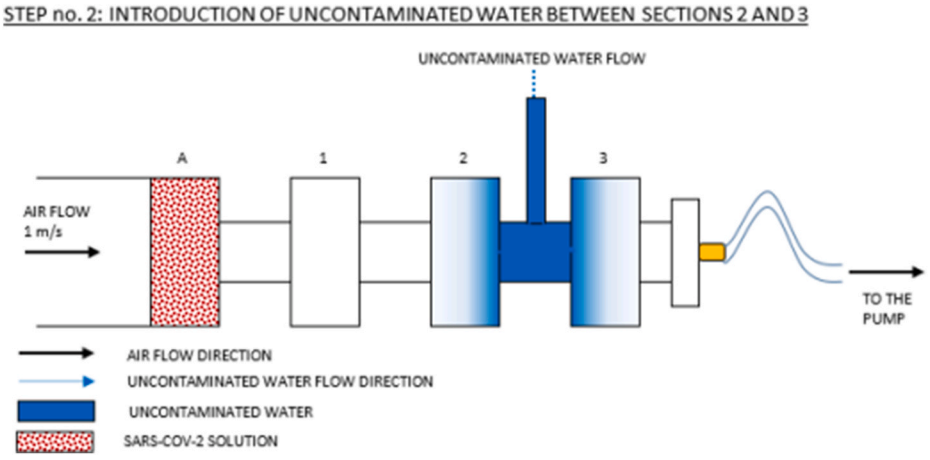

Fig. 9. Second step of the second test: introduction of the uncontaminated water between sections 2 and 3.

first demister, transversally encountering the air that was extracted from the environment via the vacuum pump, and then passed through a second demister resting on the first (Fig. 12). The first demister retains the droplets carried by the air flow. When passing through both demisters, partly thanks to the load loss when moving through these two elements, the droplets evaporate in the air flow. Compared to the second test, in this test the tunnel was maintained in horizontal position (Fig. 12). Fig. 13 is a photograph of the material used to build the two demisters and a detail of the sealing element. In this case as well, the tunnel was maintained operational (with air extraction) for the time needed for the viral solution injected inside to evaporate completely.

2.3. *Description of the experimental protocol*

To carry out the experimental tests, the protocol shown in Fig. 14 and described below was followed. Before injecting the solution containing

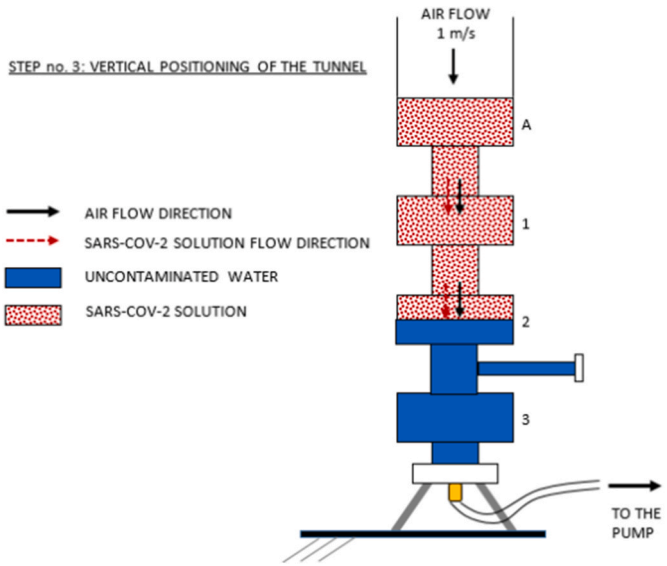

Fig. 10. Third step of the second test: vertical positioning of the tunnel.

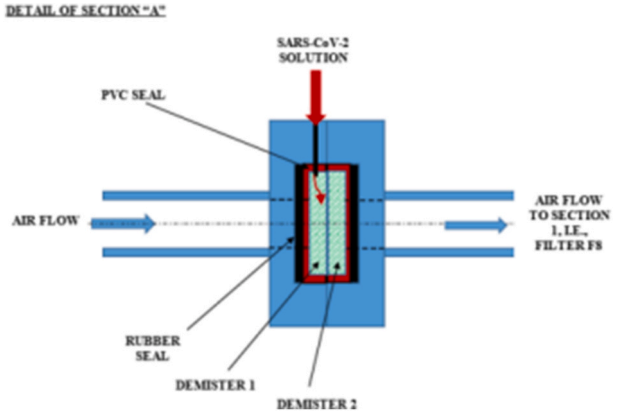

Fig. 11. Detail of section "A" implemented in the device for the third test.

SARS-CoV-2, the thermohygrometric conditions of the air in the testing environment were characterized, namely the temperature and relative humidity of the air. For this purpose, the IG-N LSI model hygrometer was used. Table 2 lists the device's main characteristics.

The velocity of the air flow in the tunnel was measured. For this purpose, the LSI Terman model hot wire anemometer was used. Table 3 lists the device's main characteristics. In the first test, the valve was set to guarantee an air velocity through the filter media equal to 0.45 m/s a value higher than the range of values used by Ref. [39]. In the second and third test, the velocity was 1 m/s. The higher filtration velocity made it possible to test conditions that are more critical for filtering efficiency. It is known from the literature that the minimum filtering efficiency of fibrous air filters decreases when filtration velocity increases [40,41].

The tunnel was then placed in a Faster BH-EN2004 Bio Safety Hood (located in a P3 laboratory) to ensure no hazardous fluids leaked out into the surrounding environment. After starting the vacuum pump, the virus-containing solution was injected into the device's entry section. The virus had been previously inactivated, i.e., made unable to replicate in cell culture, by heating to 56 °C for 30 min. Specifically, in the first test, the injected volume was a 5 cc solution with a viral concentration equal to 10^6 RNA per ml. In the second and third test, the injected volume was 2.5 cc of solution at the same viral concentration of the first

Fig. 13. The two demisters used in the experimental test.

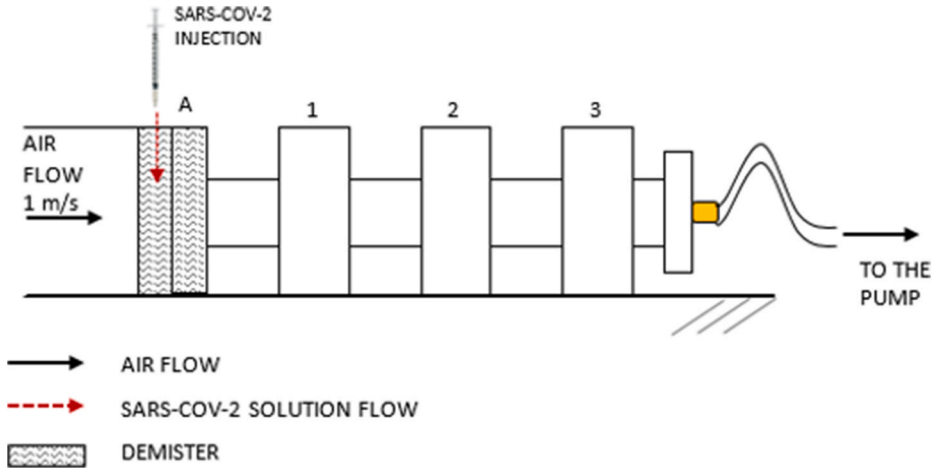

Fig. 12. Third test positioning.

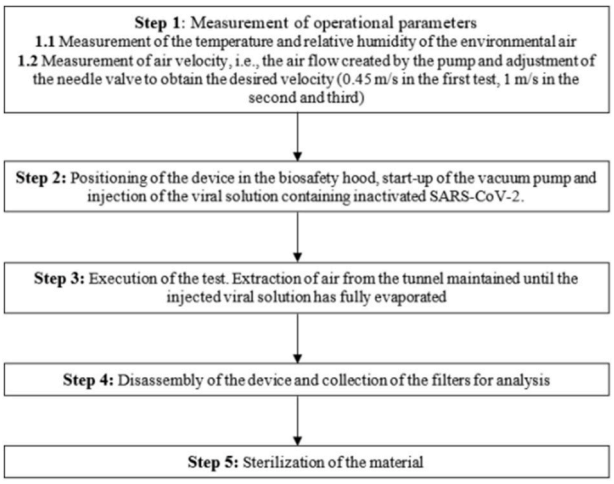

Fig. 14. Block diagram of the protocol applied in the three tests.

Table 2
Main characteristics of the IG-N model thermohygrometer.

Characteristics	Value
Sensor type	Thermistor type B
Temperature range, [°C]	[-10, 120]
Humidity range, [%]	[0, 100]

Table 3
Main characteristics of the Terman model hot wire anemometer.

Characteristics	Value
Range, [m/s]	0–15
Span, [m/s]	0–1.5
Operative temperature, [°C]	[−10, 50]
Accuracy, [%]	3%
Size	195 × 135 × 80 mm
Weight, [kg]	1.125

test.

At the end of the test, all filtering stations were disassembled and the filters collected. The first inspection was visual and its aim was to identify any abnormalities in the filtering material. In operational terms, to avoid contamination when collecting the filters, operations were started from the filtering station with the absolute filter, which, in terms of air flow, is immediately upstream of the vacuum pump. Specifically, this means station 7 in the first test and station 3 in the second and third tests. The other filters were collected moving upstream. To avoid contamination, tweezers were sterilized every time before collecting a filter. The collected filter was placed in a sterile 50 ml Falcon tube, numbered according to the filtering station in the tunnel (to ensure the traceability of the samples to analyze).

At the end of the test, to minimize the risk of contagion (despite the solution contained inactivated SARS-CoV-2), each tunnel section was soaked in a 70% alcohol solution and placed under UV-C light for 30 min, before being disposed of in compliance with local health laws.

2.4. Polymerase Chain Reaction

To check for the presence of SARS-CoV-2 RNA, each filter underwent molecular investigation using the Polymerase Chain Reaction (PCR) method.

The viral target sequences were detected using real-time RT-PCR (target: N gene), using the reference method recommended by the Centers for Disease Control and Prevention [42], after extracting the nucleic acid with the help of semi-automatic equipment (QIAsymphony SP/AS instruments, manufactured by QIAGEN, Switzerland). The detection limit of this molecular method is $10^{-0.5}$ copies RNA/µl. Every amplification test included a positive control (K+), a negative control (K-) and an extraction process control to prove that the nucleic acid had been extracted correctly and the extraction reagent was working.

2.5. Terms used

Infection is known to occur via direct and indirect contact. In the first case, viral transmission occurs directly from the infected subject to the susceptible subject, e.g. via saliva secretions released when talking, coughing or sneezing [43–45]. In the second case, contact with virus-contaminated surfaces is the source of the viral infection [46]. However, there is currently no universally accepted and scientifically established definition in the technical-scientific literature for the pathways of SARS-CoV-2 transmission and infection and, specifically, for the "droplet", "aerosol" and "airborne" pathways. In this article, as suggested by Ref. [47], we suggest using the same definitions put forward by those authors, which leave no room for doubt and distinguish, simply and clearly, between:

- *Airborne transmission*, defined as the transport of solid particles in a fluid suspension in the examined environment, in whatever way they are carried, so regardless of the carrying speed of the fluid current and therefore also including the transport of ultra-fine particles (and, as such, virions as well) subject to brownian motions;
- *Droplet transmission,* defined as the transport of droplets in the environment, regardless of how they are carried, including when they contain insoluble solid particles inside them (such as virions).

3. Results and discussion

3.1. Results of the first test

The temperature and relative humidity of the air in the first test were, respectively, 21 °C and 35.9%. With regard to Fig. 15, the filtering stations positive for the virus are shown in red, the negative ones in green. As the figure shows, only the H14 filter and the absolute filter were negative. Starting from the tunnel exit and proceeding to the entry point (i.e., from filtering station 7 to filtering station 1), the first positive filter was the F8 filter. It is therefore possible to state that the F8 filter in position 5 blocked the virus from spreading to the stations downstream. All filters upstream of the F8 filter were positive for SARS-CoV-2. The results of the test are shown in Table 4.

3.2. Results of the second test

At the end of the second test, in which the temperature and relative humidity of the air were, respectively, 21 °C and 32.4%, all the filters and the demister in section A were tested via real-time RT-PCR to check for the presence of SARS-CoV-2. As described in section 2.2.2, the filters were soaked to simulate the case that a sufficient number of droplets that hit the surfaces wet them. As shown in Fig. 17, all filters (i.e., the F8, H14 and absolute filter) were positive for SARS-CoV-2. Table 5 contains a summary of the results obtained.

3.3. Results of the third test

The temperature and relative humidity of the air in the third test were, respectively, 22 °C and 39.4%. All filters and the two demisters in section A (F8 fine filter, H14 filter and absolute filter) were subject to molecular tests to detect the presence of the SARS-CoV-2 genome.

Fig. 17 shows the stations that were positive for SARS-CoV-2 RNA in red and the negative stations in green; only the two demisters in the injection station were positive. The filters downstream of this section (i.

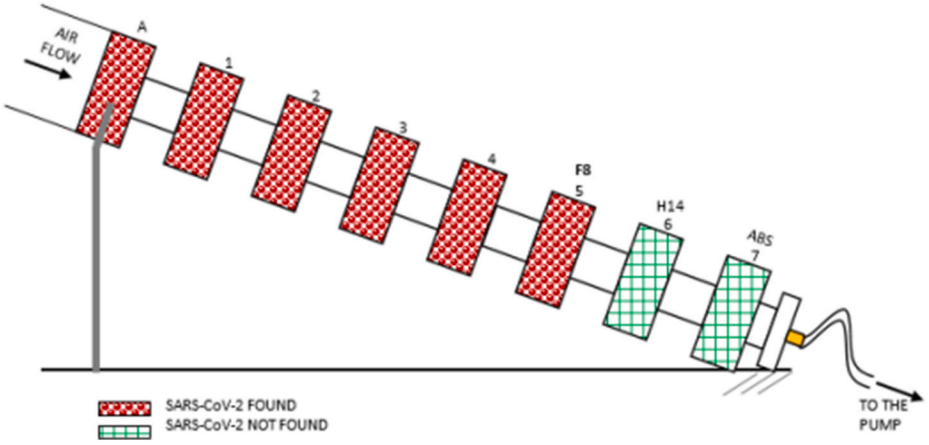

Figure 15. Graphical representation of the first test's result. The filtering stations positive for SARS-CoV-2 are shown in red, the negative ones in green. In the first test, only the H14 filter and the absolute filter were negative for SARS-CoV-2.

Table 4
Summary of the results of the first test.

Slot number	Filters	SARS-CoV-2
1	Demister	DETECTED
2	G4 pleated	DETECTED
3	G4 pleated	DETECTED
4	100% polyester fiber	DETECTED
5	F8 filter	DETECTED
6	HEPA filter	NOT DETECTED
7	Absolute filter	NOT DETECTED

Table 5
Summary of the results of the second test: wet conditions.

Slot number	Filters	SARS-CoV-2
A	Demister	DETECTED
1	F8 filter	DETECTED
2	HEPA filter	DETECTED
3	Absolute filter	DETECTED

e., the F8, H14 and absolute filters) were negative for SARS-CoV-2. A summary of the results is shown in Table 6.

3.4. Discussion on the obtained results

Briefly, the results of the three tests are as follows:

1. The first test, as shown in Fig. 15, reveals that the F8 filter was able to block the spread of the SARS-CoV-2 virus.
2. In the second test, the SARS-CoV-2 virus was detected in all stations downstream of the demister (Fig. 16). In the test, neither the F8 filter nor the H14 filter was able to block the spread of the SARS-CoV-2 virus.
3. In the third test, the SARS-CoV-2 virus was not detected in any of the filtering stations (a graphical representation of the results is shown in Fig. 17). The SARS-CoV-2 was found only in the entry station, i.e., in the two demisters.

Table 6
Summary of the results of the third test: wet conditions.

Slot number	Filters	SARS-CoV-2
A	Two Demisters	DETECTED IN BOTH
1	F8 filter	NOT DETECTED
2	HEPA filter	NOT DETECTED
3	Absolute filter	NOT DETECTED

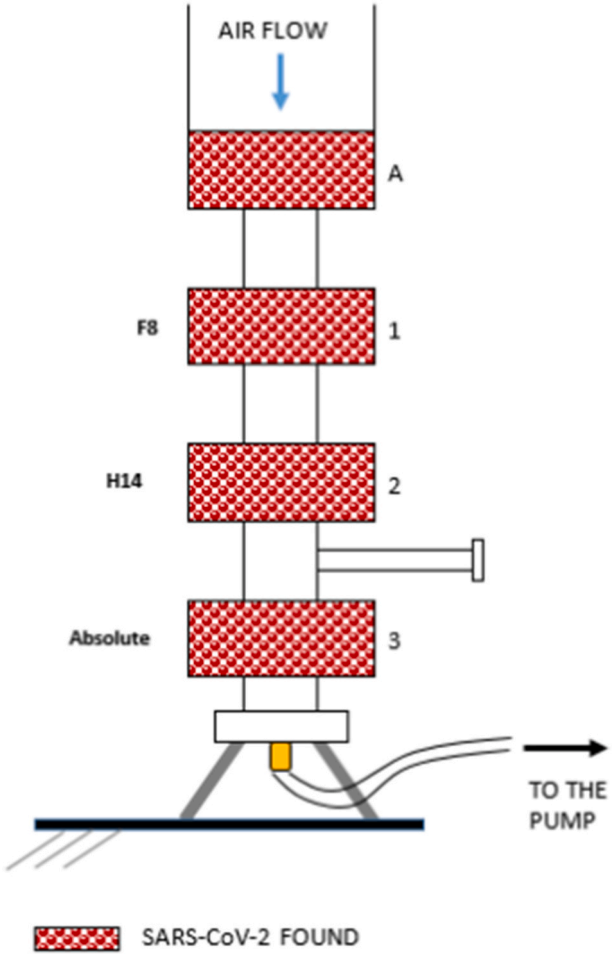

Fig. 16. Graphical representation of the second test's result. The filtering stations positive for SARS-CoV-2 are shown in red, the negative ones in green. All filters were positive.

Based on the test results, it can be said that the F8 filter blocks SARS-CoV-2 propagation if it encounters a flow devoid of liquid phase, i.e., a biphasic flow that can wet the filtering material. In the first test, the system allowed the complete evaporation of the solution containing SARS-CoV-2 before it reached the F8 filter, which blocked the virus from spreading to the downstream filters. As schematically shown in Fig. 18,

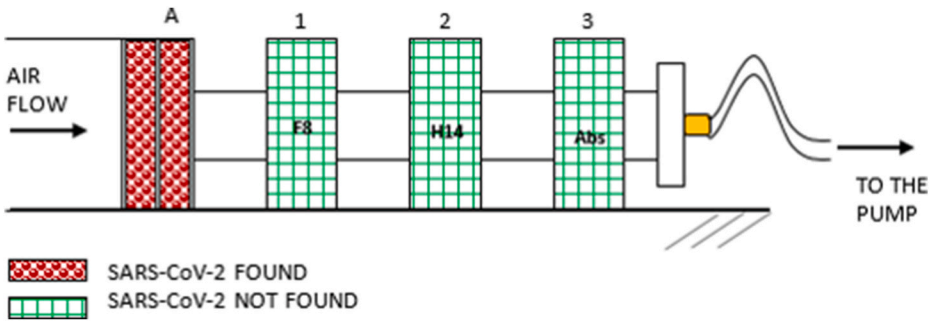

Fig. 17. Graphical representation of the third test's result. The filtering stations positive for SARS-CoV-2 are shown in red, the negative ones in green. Only the two demisters in station A were positive for SARS-CoV-2.

the evaporation of the injected fluid allows the switch from a droplet-type transmission (i.e., virions in droplets) to an airborne transmission before the F8 filter. Because SARS-CoV-2 was detected in stations 1–4, it can be said that the virus came into contact with the filtering material because it was carried either inside droplets or on dried particles.

As shown in the second test, if the amount of droplets in the flow hitting the F8 filter (or the F14 filter) were enough to wet it, then both filter faces (and the downstream one in particular) would be wet and viral transmission downstream would be possible. Fig. 19 shows how, if the filtering surface is wet, the SARS-CoV-2 virus propagates and moves through all 3 filtering stations downstream of the demister.

The third test shows that, if the infected droplets do not move beyond the section containing the demisters (which can be considered very coarse filters), the viral load stops there. Specifically, the larger droplets are blocked by the demister and evaporate; the smaller ones, which could cross through, evaporate before exiting the demister, as shown in Fig. 20. In the picture, the black dots are a schematic representation of the virions that are likely deposited on the demister after the evaporation of the injected liquid.

Although there is no consensus in the literature when describing what happens to the solid residue and to the viral content when the droplets evaporate [48], it can be reasonably assumed that the droplets that dry on the demister leave a solid residue there and, very probably, viral load. In the third test, as there were no traces of virus in the downstream filters and, in particular, in the F8 filter, the solid residue and the viral content were trapped in the demisters in station A.

However, this experimental result must be analyzed considering the short duration of the experiment and the fact that the solution with SARS-CoV-2 was injected very rapidly at the beginning of the test. Over longer periods (i.e., when droplets enter over a more extended time interval), it is reasonable to hypothesize that an accumulation of virus-containing solid residues on the demister fibers may, at some point, lead to the particles detaching from the demister. In this case, the solid residues could move and hence affect the filtering stations downstream. However, as shown in the first test, if the air flow does not have a liquid phase that can wet both sides of the F8 filter, the filter can block the propagation of dried nuclei, even if, in real life applications, the use of an H14 filter is recommended.

Lastly, it is important to note one last finding from the third test. The increase in pressure drop in section A resulting from the presence of the two demisters had a positive effect on the evaporation of the injected solution. The total pressure downstream of the station is equal to the environmental pressure minus the pressure drop in the station. Therefore, the greater the pressure drop, the lower the total pressure. Lower pressure is accompanied by an increase in the moisture content in saturated conditions. Therefore, all other thermohygrometric conditions being equal, the increase in pressure drops leads to moving away from saturation conditions, i.e., leads to conditions that favour the complete evaporation of the infected droplet, as long as the flow of liquid is not such that saturation conditions are ensured in every section of the testing tunnel. This occurs because, at the same air flow velocity, the droplet's lifetime, i.e., the distance covered before it evaporates completely, decreases. Therefore, the presence of the demister does not just block the larger droplets, it also acts by reducing the lifetime of the smaller droplets, i.e., it creates protection for the more performing air filters that, if wet, would allow the virus to move downstream.

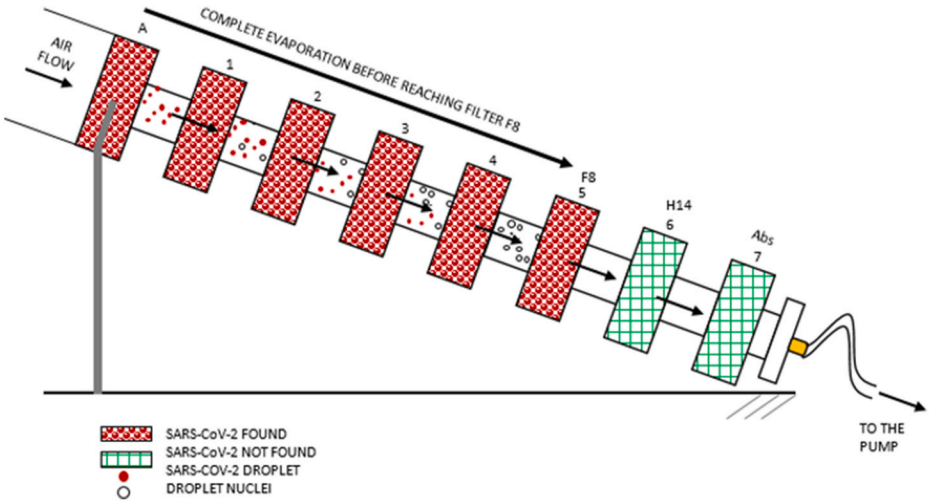

Fig. 18. Graphical representation of the first test's result.

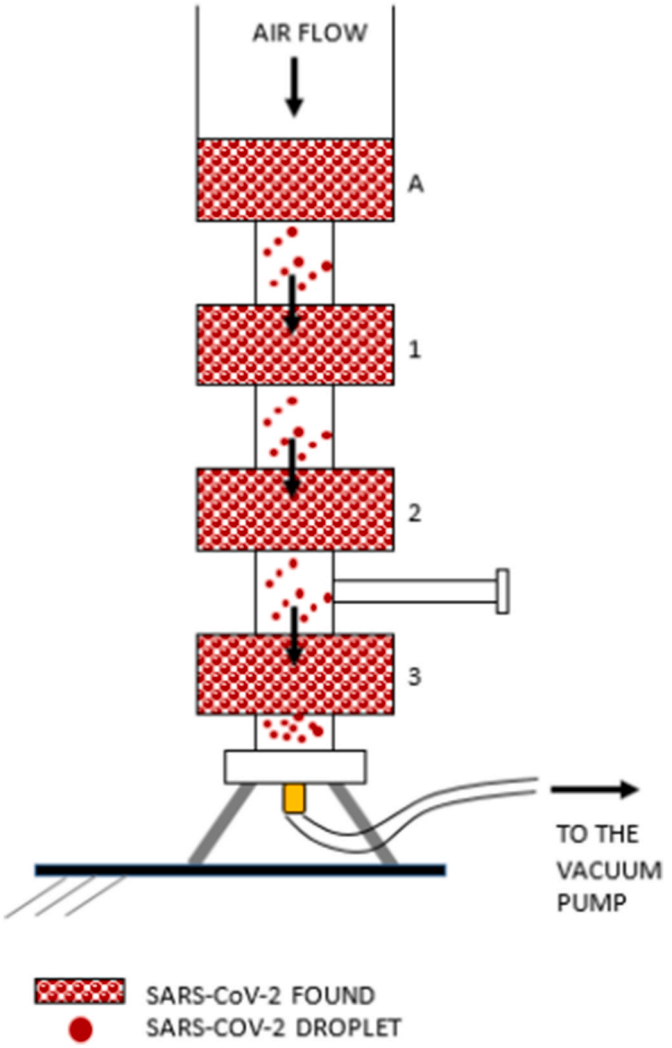

Fig. 19. Graphical representation of the second test's result. All the filters were soaked to simulate a wetted filters' surfaces.

3.5. Good practices for the design and operation of filtering section in HVAC system against SARS-CoV-2 propagation

Based on the terms introduced in section 2.5 and the experimental results, it is possible to provide indications of improving the performance of filtration systems installed in HVAC systems against the spread of the SARS-CoV-2 virus.

The first intervention to be carried out on HVAC systems is installing a demister section upstream of a high-performance filter. The demister section is cheap and easily installable even in existing systems, where the available spaces are often minimal. The demister section guarantees the following benefits: firstly, it blocks the largest droplets that carry, on average, the greatest number of virions. Secondly, it protects the downstream filtering section (i.e., the high-efficiency filter) from being wet, i.e., losing the capacity to block SARS-CoV-2 as demonstrated by the second test. Thirdly, the demister section causes a pressure drop that eases the complete evaporation (from droplet to airborne transmission) before the downstream filter of the smallest droplets that pass through the demister. As validated in the third test, the complete evaporation of the smaller droplets minimizes the risk of wetting of the high-performance filter placed downstream.

The high-performance filter's installation is critical, especially for existing HVAC systems where dimensions, pressure drops, costs are limiting conditions during the selection. According to the experimental results, the second filtering section should consist of a F8 or a higher filtering performance filter that, if not wet, prevents the propagation of SARS-CoV-2. The experimental results can be considered by end-users selecting the high-efficiency filter based on design and operation requirements. From a technical point of view, installing a H14 instead of a F8 would be the best choice since the H14 filter would ensure high filtering efficiency. At the same time, high HVAC system performances for its correct operation are required.

However, it is not always possible to install a H14 filter, especially in revamping existing filtering systems. Installing a filter other than the one for which the HVAC system is designed and certified involves an off-design if not appropriately counterbalanced with other technical changes to the system. If not counterbalanced, the control of the air thermo-hygrometric conditions is negatively impacted. However, also the thermo-hygrometric conditions control is an essential condition to minimize the spread of the SARS-CoV-2 virus infection [47,49].

4. Conclusions

The experimental campaign provided useful information for the running and ex-novo design of air conditioning facilities during the SARS-CoV-2 pandemic and for potential new pandemic waves spreading in similar patterns, in particular in terms of the filtering section.

A good practice to adopt, to minimize the propagation of SARS-CoV-2 in air conditioning systems, is to use a configuration that is typically found in industrial mechanical facilities, which consist in having a coarse filter followed by finer filter(s) downstream. Installing only a high performance filter in the air conditioning facility (such as an H14 filter), does not guarantee that SARS-CoV-2 propagation is blocked, as shown by the results of test 2, i.e., if the filter surfaces become wet.

A good practice for the design and the operation of the filtering section of the air conditioning unit must include:

- A coarse filter installed to protect the fine filter downstream.

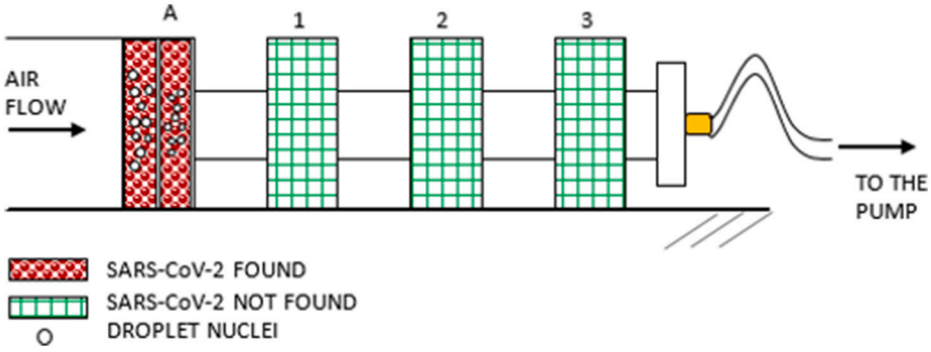

Fig. 20. Graphical representation of the third test's result.

The purpose of the preliminary coarse filter is to block the movement of infected droplets before they come into contact with the fine filter or the absolute filter downstream (and wetting their surfaces), which makes these filters ineffective in stopping SARS-CoV-2 propagation (as shown by the results of the second experimental test). As can be deduced from the third test, while the larger droplets are blocked by the filtering material, where they deposit and evaporate, leaving a reasonably infected solid residue, the smaller droplets that are not captured by the filter evaporate completely in the air before reaching the higher performing filter downstream.

- A filter (fine class, minimum) with the purpose of stopping the motion of any infected solid nuclei that could be released by the coarse filter upstream.

As shown in the first test, filters with filtering performance equal to or greater than the F8 filter block SARS-CoV-2 propagation if they encounter a flow devoid of liquid phase. Therefore, even if after prolonged activity periods, some solid nuclei do detach from the coarse filter, the fine filter acts as barrier, preventing the release of the SARS-CoV-2 virus into the environment the conditioned air is pumped into.

CRediT authorship contribution statement

Cesare Saccani: Writing – review & editing, Writing – original draft, Supervision, Methodology, Investigation, Formal analysis, Conceptualization. **Alessandro Guzzini:** Writing – review & editing, Writing – original draft, Methodology, Investigation, Data curation. **Caterina Vocale:** Supervision, Methodology, Investigation, Formal analysis. **Davide Gori:** Writing – review & editing, Investigation. **Marco Pellegrini:** Writing – review & editing, Methodology, Investigation. **Maria Pia Fantini:** Writing – review & editing. **Alessandra Primavera:** Investigation.

Declaration of competing interest

The authors declare that they have no known competing financial interests or personal relationships that could have appeared to influence the work reported in this paper.

Acknowledgement

The Authors acknowledge the local public transport company TPER (Trasporto Passeggeri Emilia Romagna), which financed the research activities.

References

[1] A.D. Kaye, C.N. Okeagu, A.D. Pham, R.A. Silva, J.J. Hurley, B.L. Arron, N. Sarfraz, H.N. Lee, G.E. Ghali, J.W. Gamble, H. Liu, R.D. Urman, E.M. Cornett, Economic impact of COVID-19 pandemic on healthcare facilities and systems: international perspectives, Best Pract. Res. Clin. Anaesthesiol. 35 (2021) 293–306, https://doi.org/10.1016/J.BPA.2020.11.009.

[2] V. Auriemma, C. Iannaccone, COVID-19 pandemic: socio-economic consequences of social distancing measures in Italy, Front. Sociol. (2020) 78, https://doi.org/10.3389/FSOC.2020.575791, 0.

[3] M. Mazza, G. Marano, C. Lai, L. Janiri, G. Sani, Danger in danger: interpersonal violence during COVID-19 quarantine, Psychiatr. Res. 289 (2020) 113046, https://doi.org/10.1016/j.psychres.2020.113046.

[4] M. Nicola, Z. Alsafi, C. Sohrabi, A. Kerwan, A. Al-Jabir, C. Iosifidis, M. Agha, R. Agha, The socio-economic implications of the coronavirus pandemic (COVID-19): a review, Int. J. Surg. 78 (2020) 185–193, https://doi.org/10.1016/j.ijsu.2020.04.018.

[5] L. Sher, The impact of the COVID-19 pandemic on suicide rates, QJM An Int. J. Med. (2020), https://doi.org/10.1093/qjmed/hcaa202.

[6] D. Zhang, M. Hu, Q. Ji, Financial markets under the global pandemic of COVID-19, Finance Res. Lett. (2020) 101528, https://doi.org/10.1016/j.frl.2020.101528.

[7] K. Azuma, U. Yanagi, N. Kagi, H. Kim, M. Ogata, M. Hayashi, Environmental factors involved in SARS-CoV-2 transmission: effect and role of indoor environmental quality in the strategy for COVID-19 infection control, Environ. Health Prev. Med. 251 (25) (2020) 1–16, https://doi.org/10.1186/S12199-020-00904-2, 2020.

[8] U. Ranga, SARS-CoV-2 aerosol and droplets: an overview, VirusDisease 2021 322 (32) (2021) 190–197, https://doi.org/10.1007/S13337-021-00660-Z.

[9] S.Y. Park, Y.M. Kim, S. Yi, S. Lee, B.J. Na, C.B. Kim, J. Il Kim, H.S. Kim, Y.B. Kim, Y. Park, I.S. Huh, H.K. Kim, H.J. Yoon, H. Jang, K. Kim, Y. Chang, I. Kim, H. Lee, J. Gwack, S.S. Kim, M. Kim, S. Kweon, Y.J. Choe, O. Park, Y.J. Park, E.K. Jeong, Coronavirus disease outbreak in call center, South Korea, Emerg, Inf. Disp. 26 (2020) 1666–1670, https://doi.org/10.3201/eid2608.201274.

[10] J. Lu, J. Gu, J. Gu, K. Li, C. Xu, W. Su, Z. Lai, D. Zhou, C. Yu, B. Xu, Z. Yang, COVID-19 outbreak associated with air conditioning in restaurant, Guangzhou, China, 2020, Emerg. Infect. Dis. 26 (2020) 1628–1631, https://doi.org/10.3201/eid2607.200764.

[11] Y. Shen, C. Li, H. Dong, Z. Wang, L. Martinez, Z. Sun, A. Handel, Z. Chen, E. Chen, M.H. Ebell, F. Wang, B. Yi, H. Wang, X. Wang, A. Wang, B. Chen, Y. Qi, L. Liang, Y. Li, F. Ling, J. Chen, G. Xu, Community outbreak investigation of SARS-CoV-2 transmission among bus riders in Eastern China, JAMA Intern. Med. (2020), https://doi.org/10.1001/jamainternmed.2020.5225.

[12] C. Ou, S. Hu, K. Luo, H. Yang, J. Hang, P. Cheng, Z. Hai, S. Xiao, H. Qian, S. Xiao, X. Jing, Z. Xie, H. Ling, L. Liu, L. Gao, Q. Deng, B.J. Cowling, Y. Li, Insufficient ventilation led to a probable long-range airborne transmission of SARS-CoV-2 on two buses, Build. Environ. 207 (2022) 108414, https://doi.org/10.1016/J.BUILDENV.2021.108414.

[13] Ontario Agency for Health Protection and Promotion (Public Health Ontario), COVID-19 Transmission from Singing and Playing Wind Instruments-What We Know So Far 1 SYNOPSIS Updates to Our, Latest Version, Toronto, 2020.

[14] J.J. Herstein, A. Degarege, D. Stover, C. Austin, M.M. Schwedhelm, J. Lawler, J. J. Lowe, A.K. Ramos, M. Donahue, Characteristics of SARS-CoV-2 transmission among meat processing workers in Nebraska, USA, and effectiveness of risk mitigation measures, Emerg. Infect. Dis. 27 (2021), https://doi.org/10.3201/eid2704.204800.

[15] H. Qian, T. Miao, L. Liu, X. Zheng, D. Luo, Y. Li, Indoor Transmission of SARS-CoV-2, Preprint, 2020, https://doi.org/10.1101/2020.04.04.20053058.

[16] REHVA, How to Operate and Use Building Services in Order to Prevent the Spread of the Coronavirus Disease (COVID-19) Virus (SARS-CoV-2) in Workplaces, 2020.

[17] AICARR, COVID-19. https://www.aicarr.org/Pages/Normative/FOCUS_COVID-19_IT.aspx, 2020. (Accessed 10 December 2020).

[18] J. Lawrence, J. Shoen, A S H R A E J O U guidance for building operations during the COVID-19 pandemic, ASHRAE J. (2020), https://doi.org/10.1056/NEJMc2004973.

[19] S. Zhang, Z. Ai, Z. Lin, Occupancy-aided ventilation for both airborne infection risk control and work productivity, Build. Environ. 188 (2021) 107506, https://doi.org/10.1016/j.buildenv.2020.107506.

[20] L.F. Pease, N. Wang, T.I. Salsbury, R.M. Underhill, J.E. Flaherty, A. Vlachokostas, G. Kulkarni, D.P. James, Investigation of potential aerosol transmission and infectivity of SARS-CoV-2 through central ventilation systems, Build. Environ. 197 (2021) 107633, https://doi.org/10.1016/j.buildenv.2021.107633.

[21] ISO, ISO 29463-1:2017, High Efficiency Filters and Filter Media for Removing Particles from Air — Part 1: Classification, Performance, Testing and Marking, 2017. https://www.iso.org/obp/ui/#iso:std:iso:29463:-1:ed-2:v1:en. (Accessed 10 December 2020).

[22] N. Zhu, D. Zhang, W. Wang, X. Li, B. Yang, J. Song, X. Zhao, B. Huang, W. Shi, R. Lu, P. Niu, F. Zhan, X. Ma, D. Wang, W. Xu, G. Wu, G.F. Gao, W. Tan, A novel coronavirus from patients with pneumonia in China, 2019, N. Engl. J. Med. 382 (2020) 727–733, https://doi.org/10.1056/NEJMoa2001017.

[23] A. Hammond, T. Khalid, H.V. Thornton, C.A. Woodall, A.D. Hay, Should homes and workplaces purchase portable air filters to reduce the transmission of SARS-CoV-2 and other respiratory infections? A systematic review, PLoS One 16 (2021), e0251049, https://doi.org/10.1371/JOURNAL.PONE.0251049.

[24] P.F. Horve, L.G. Dietz, M. Fretz, D.A. Constant, A. Wilkes, J.M. Townes, R. G. Martindale, W.B. Messer, K.G. Van Den Wymelenberg, Identification of SARS-CoV-2 RNA in healthcare heating, ventilation, and air conditioning units, Indoor Air (2021), https://doi.org/10.1111/INA.12898.

[25] J. Gralton, E. Tovey, M.L. McLaws, W.D. Rawlinson, The role of particle size in aerosolised pathogen transmission: a review, J. Infect. 62 (2011) 1–13, https://doi.org/10.1016/j.jinf.2010.11.010.

[26] D.A. Christopherson, W.C. Yao, M. Lu, R. Vijayakumar, A.R. Sedaghat, High-efficiency particulate air filters in the era of COVID-19: function and efficacy, Otolaryngol. Head Neck Surg. 163 (2020) 1153–1155, https://doi.org/10.1177/0194599820941838.

[27] B. Elias, Y. Bar-Yam, Could air filtration reduce COVID-19 severity and spread? New Engl. Complex Syst. Inst. (2020). https://necsi.edu/could-air-filtration-reduce-covid19-severity-and-spread. (Accessed 10 December 2020).

[28] Z. Feng, S.J. Cao, F. Haghighat, Removal of SARS-CoV-2 using UV+Filter in built environment, Sustain. Cities Soc. 74 (2021) 103226, https://doi.org/10.1016/J.SCS.2021.103226.

[29] T. Sandle, Review of the efficacy of HEPA filtered air to control coronavirus risks in cleanrooms, Eur. J. Parenter. Pharm. Sci. 252 (2020), https://doi.org/10.37521/25203.

[30] S. Yeo, I. Hosein, L. McGregor-Davies, Use of HEPA filters to reduce the risk of nosocomial spread of SARS-CoV-2 via operating theatre ventilation systems, Br. J. Anaesth. 125 (2020), https://doi.org/10.1016/j.bja.2020.07.013 e361–e363.

[31] J. Zhang, D. Huntley, A. Fox, B. Gerhardt, A. Vatine, J. Cherne, Study of viral filtration performance of residential HVAC filters, ASHRAE J. (2020). www.ashrae.org. (Accessed 14 June 2021).

[32] N. Zacharias, A. Haag, R. Brang-Lamprecht, J. Gebel, S.M. Essert, T. Kistemann, M. Exner, N.T. Mutters, S. Engelhart, Air filtration as a tool for the reduction of viral aerosols, Sci. Total Environ. 772 (2021) 144956, https://doi.org/10.1016/j.scitotenv.2021.144956.
[33] J.B. Harstad, H.M. Decker, L.M. Buchanan, M.E. Filler, Air filtration of submicron virus aerosols, Am. J. Publ. Health Nation's Health 57 (1967) 2186–2193, https://doi.org/10.2105/AJPH.57.12.2186.
[34] P. Roelants, B. Boon, W. Lhoest, Evaluation of a commercial air filter for removal of viruses from the air, Appl. Microbiol. 16 (1968) 1465–1467, https://doi.org/10.1128/aem.16.10.1465-1467.1968.
[35] M. Mrozek', U. Zillmann', W. Nicklas', V. Kraft, B. Meyer, E. Sickel, B. Lehr', A. Wetzel2, Efficiency of air filter sets for the prevention of airborne infections in laboratory animal houses, Lab. Anim. 28 (1993) 347–354.
[36] J.E. Farnsworth, S.M. Goyal, S. Won Kim, T.H. Kuehn, P.C. Raynor, M. A. Ramakrishnan, S. Anantharaman, W. Tang, Development of a method for bacteria and virus recovery from heating, ventilation, and air conditioning (HVAC) filters, J. Environ. Monit. 8 (2006) 1006–1013, https://doi.org/10.1039/b606132j.
[37] N.C. Burton, S.A. Grinshpun, T. Reponen, Physical collection efficiency of filter materials for bacteria and viruses, Ann. Occup. Hyg. 51 (2007) 143–151, https://doi.org/10.1093/annhyg/mel073.
[38] C. Wenke, J. Pospiech, T. Reutter, U. Truyen, S. Speck, Efficiency of different air filter types for pig facilities at laboratory scale, PLoS One 12 (2017), https://doi.org/10.1371/journal.pone.0186558.
[39] B. Shi, L.E. Ekberg, S. Langer, Intermediate air filters for general ventilation applications: an experimental evaluation of various filtration efficiency expressions, Aerosol Sci. Technol. 47 (2013) 488–498, https://doi.org/10.1080/02786826.2013.766667/SUPPL_FILE/UAST_A_766667_SUP_31577572.ZIP.
[40] K.W. Lee, B.Y.H. Liu, On the minimum efficiency and the most penetrating particle size for fibrous filters, J. Air Pollut. Control Assoc. 30 (1980) 377–381, https://doi.org/10.1080/00022470.1980.10464592.
[41] D. Sinclair, Penetration of hepa filters by submicron aerosols, J. Aerosol Sci. 7 (1976) 175–179, https://doi.org/10.1016/0021-8502(76)90073-2.
[42] CDC, CDC 2019-Novel Coronavirus (2019-nCoV) Real-Time RT-PCR Diagnostic Panel, Centers Dis. Control Prev, 2020. https://www.fda.gov/media/134922/download.
[43] X. Peng, X. Xu, Y. Li, L. Cheng, X. Zhou, B. Ren, Transmission routes of 2019-nCoV and controls in dental practice, Int. J. Oral Sci. 12 (2020) 1–6, https://doi.org/10.1038/s41368-020-0075-9.
[44] S. Asadi, N. Bouvier, A.S. Wexler, W.D. Ristenpart, Aerosol Science and Technology the coronavirus pandemic and aerosols: does COVID-19 transmit via expiratory particles? Aerosol Sci. Technol. 54 (2020) 635–638, https://doi.org/10.1080/02786826.2020.1749229.
[45] M. Jayaweera, H. Perera, B. Gunawardana, J. Manatunge, Transmission of COVID-19 virus by droplets and aerosols: a critical review on the unresolved dichotomy, Environ. Res. 188 (2020) 109819, https://doi.org/10.1016/j.envres.2020.109819.
[46] N. van Doremalen, T. Bushmaker, D.H. Morris, M.G. Holbrook, A. Gamble, B. N. Williamson, A. Tamin, J.L. Harcourt, N.J. Thornburg, S.I. Gerber, J.O. Lloyd-Smith, E. de Wit, V.J. Munster, Aerosol and surface stability of SARS-CoV-2 as compared with SARS-CoV-1, N. Engl. J. Med. 382 (2020) 1564–1567, https://doi.org/10.1056/nejmc2004973.
[47] C. Saccani, M.P. Fantini, D. Gori, A. Guzzini, M. Pellegrini, M.C. Re, C. Reno, G. Roncarati, C. Vocale, Analisi della trasmissione di SARS-CoV-2: influenza delle condizioni termoigrometriche rispetto al rischio di diffusione del contagio - AMS Acta - AlmaDL Università di Bologna, AMS ACTA, 2020. http://amsacta.unibo.it/6521/. (Accessed 9 December 2020).
[48] Z. He, S. Shao, J. Li, S.S. Kumar, J.B. Sokoloff, J. Hong, Droplet evaporation residue indicating SARS-COV-2 survivability on surfaces, Phys. Fluids 33 (2021), https://doi.org/10.1063/5.0038562.
[49] C. Saccani, Il controllo dell'umidità dell'aria: ecco perchè è decisivo contro il contagio, Lettera 150 (2) (2020) 23–36.